Towards J/mol Accuracy for the Cohesive Energy of Solid Argon

Peter Schwerdtfeger,* Ralf Tonner, Gloria E. Moyano, and Elke Pahl

Abstract: *The cohesive energies of argon in its cubic and hexagonal closed packed structures are computed with an unprecedented accuracy of about 5 J mol^{-1} (corresponding to 0.05 % of the total cohesive energy). The same relative accuracy with respect to experimental data is also found for the face-centered cubic lattice constant deviating by ca. 0.003 Å. This level of accuracy was enabled by using high-level theoretical, wave-function-based methods within a many-body decomposition of the interaction energy. Static contributions of two-, three-, and four-body fragments of the crystal are all individually converged to sub-J mol^{-1} accuracy and complemented by harmonic and anharmonic vibrational corrections. Computational chemistry is thus achieving or even surpassing experimental accuracy for the solid-state rare gases.*

*I*t is currently a challenge for computational chemistry to calculate dissociation energies to an accuracy of 1 kJ mol^{-1} or better for simple molecules when compared to high precision measurements.[1–5] It is even a greater challenge to reach such accuracies for the solid state,[6–9] often required to correctly describe the energy separation between different polymorphs and to predict the correct crystalline ground state.[10] John Maddox noted in 1988 that "one of the continuing scandals in the physical sciences" is that "it remains in general impossible to predict the structure of even the simplest crystalline solids from a knowledge of their chemical composition."[11] This statement is perhaps still valid almost 30 years later,[12] although recent progress in the ab initio treatment of condensed phases starts to show very promising results.[9,13,14] The importance of being able to describe polymorphism accurately is not only of theoretical interest but also critical to applications, for example, in the development of pharmaceutical compounds.

The so-called "rare gas problem" is one striking example for energetically close-lying polymorphs with the face-centered cubic (fcc) and the hexagonal closed-packed (hcp) structures being almost isoenergetic. Nevertheless, the fcc lattice is found predominantly—and not the hcp or any mixture of closed-packed layers (Barlow packings). The hcp structure has been observed only in freshly frozen argon by Barrett and Meyer as a metastable phase.[15,16] Under very high pressures a phase transition from fcc to hcp structures is expected for the rare gases, the exact transition pressure is still being debated and probably lies in the range of several to tens of GPa. Many questions remain unanswered: Why does nature prefer fcc lattices? What are possible crystal growth mechanisms leading to the observed fcc structures? At what pressures does the fcc–hcp phase transition occur? The basis to tackle such questions is the ability to obtain accurate cohesive energies at zero Kelvin. Here, we will show how to achieve this goal for the argon crystal aiming at a J mol^{-1} accuracy.

Wave-function-based methods that include electron correlation have already been successfully applied to these kinds of problems. One example is the incremental method, which consists of a many-body expansion of the interaction energy.[17–19] The method has even been applied for a few selected metallic systems.[20,21] Within the many-body decomposition one divides the problem of calculating the total interaction energy (of *N* atoms) into the contributions of all possible dimers, trimers, and larger (embedded) fragments. Convergence of this expansion can be achieved when the importance of the larger fragments decreases quickly.

For rare gases the many-body expansion is known to converge fast under ambient conditions (i.e. in the low-pressure and -temperature range), thus providing an ideal test case for accurate quantum chemical methods. Calculating the many-body terms with accurate relativistic coupled-cluster data, one obtains impressive results for rare-gas solid-state properties, phase transitions, and the equation of state.[13,22–29] The slight preference of the closed packed fcc over the hcp lattice structure was recently proposed to be due to zero-point vibrational effects beyond the Einstein approximation and in the J mol^{-1} range.[13,30] It is clear that such small energy differences for different polymorphs in a solid can currently not be obtained from standard density functional theory commonly used in solid-state calculations,[10] even if dispersion-correction schemes are introduced.[31] Hence sophisticated wave-function-based methods are required. This, however, becomes a daunting task even for rare-gas crystals as we shall see.

Here, we investigate the fcc and hcp polymorphs of argon by adding all important *n*-body contributions to the cohesive energy and to the lattice parameters (at 0 K). The total cohesive energy per atom $E_{coh}(V)$ depends on the volume *V* of the unit cell via the lattice constant. It can be divided into

[*] Prof. Dr. P. Schwerdtfeger
Centre for Theoretical Chemistry and Physics, The New Zealand Institute for Advanced Study, Massey University Auckland
Private Bag 102904, 0632 Auckland (New Zealand)
E-mail: p.a.schwerdtfeger@massey.ac.nz

Dr. R. Tonner
Fachbereich Chemie, Philipps-Universität Marburg
Hans-Meerwein-Str. 4, 35032 Marburg (Germany)

Dr. G. E. Moyano
Instituto de Química, Universidad de Antioquia
AA 1126 Medellín (Colombia)

Dr. E. Pahl
Centre for Theoretical Chemistry and Physics, Institute for Natural and Mathematical Sciences, Massey University Auckland
Private Bag 102904, 0632 Auckland (New Zealand)

The ORCID identification number(s) for the author(s) of this article can be found under http://dx.doi.org/10.1002/anie.201605875.

static $E_{coh}^{stat}(V)$ and dynamic $E_{coh}^{dyn}(V)$ contributions, the latter resulting from zero-point vibrational motion [Eq. (1)].

$$E_{coh} = E_{coh}^{stat}(V) + E_{coh}^{dyn}(V) \tag{1}$$

The total static contribution is approximated within the many-body ansatz including two-, three-, and four-body contributions $E^{(n)}(V)$ plus the two-component (2C) contribution $E_{2C}^{(2)}(V)$ describing mostly spin-orbit effects [Eq. (2)].

$$E_{coh}^{stat}(V) \cong E^{(2)}(V) + E^{(3)}(V) + E^{(4)}(V) + E_{2C}^{(2)}(V) \tag{2}$$

Here we use translational symmetry to evaluate $E^{(n)}(V)$; for example, for the two-body contribution we sum over all individual $\Delta E^{(2)}(R_{0i})$ terms from a (arbitrarily) chosen reference atom at position R_{0i} to all other atoms in the crystal. The individual n-body potentials $\Delta E^{(n)}(R)$ are shown in Figure 1. For a detailed discussion on the accuracy of the two- and three-body potentials see Refs. [32–34].
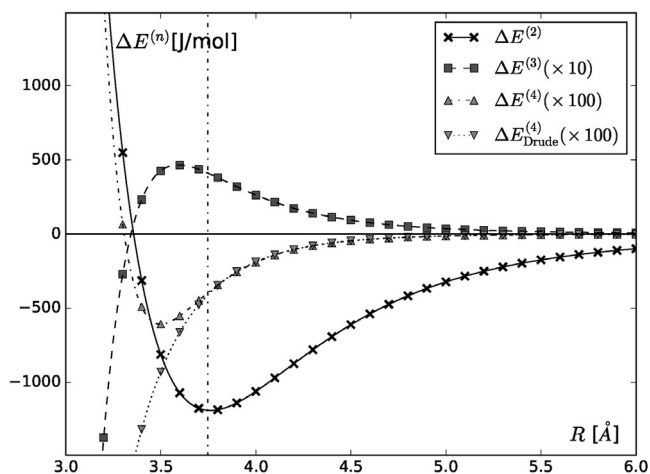

Figure 1. n-Body energy contributions $\Delta E^{(n)}(R)$ (in J mol^{-1}) as a function of the internuclear distance R (in Å). The two-body potential is from Jäger et al.[32] and the three-body term from Cencek et al.[34] Note that the three-body contribution is scaled by a factor of 10 and the four-body contribution by a factor of 100 for better visibility. For the three-body term an equilateral triangle is chosen, and an ideal tetrahedron for the four-body term. The four-body term is derived from relativistic CCSD(T) calculations and for comparison is shown together with the long-range Drude model. The experimental nearest-neighbor distance for solid argon[38] extrapolated to 0 K is shown as a dashed vertical line.

As can be seen in Figure 1, the higher n-body contributions $\Delta E^{(n)}$ become successively smaller by more than one order of magnitude each with increasing order n and so do the total $E^{(n)}$ terms. This is the reason for the fast convergence to the exact cohesive energy for rare gases such as argon and the justification for truncating the expansion at the fourth-order term as shown in Equation (2). The fifth-order contributions can be estimated to amount to less than 0.1 J mol^{-1}. We also note that the three- and four-body terms around the nearest-neighbor distance of solid argon (3.7560 Å for the fcc structure)[15] are well described by Drude's classical dispersion model.[35,36] Further, all curves go through zero close to

the hard-sphere radius R_2=3.3574 Å defined by $\Delta E^{(2)}(R_2) = 0$. We find $\Delta E^{(3)}(R_3) = 0$ at $R_3 = 3.3436$ Å and $\Delta E^{(4)}(R_4) = 0$ at $R_4 = 3.3127$ Å, and we observe that $R_2 > R_3 > R_4$. We also mention that the three most accurate two-body potentials available have quite similar properties: for the equilibrium bond distance r_e, potential depth D_e, and hard-sphere radius R_2 we get for the Jäger et al. (JHBV) potential (shown in Figure 1) $r_e = 3.7618$ Å, $D_e = 1190.0$ J mol^{-1}, $R_2 = 3.3574$ Å,[32] for the Patkowski and Szalewicz (PS) potential $r_e = 3.7624$ Å, $D_e = 1188.5$ J mol^{-1}, $R_2 = 3.3577$ Å,[32] and for the Aziz (Az) potential $r_e = 3.7570$ Å, $D_e = 1190.9$ J mol^{-1}, $R_2 = 3.3502$ Å.[37] The empirical Aziz potential is fitted to vibrational–rotational data and has a shorter bond distance than that of the two ab initio curves.[37]

A first approximation for the dynamic zero-point energy (ZPE) effects is given within the Einstein approximation (ZPE-E) where one looks at the contributions when one atom is moved in the potential created by the rest of the atoms fixed at their original positions. The effects on the two- and three-body contributions can be approximated by a harmonic potential or treated more accurately by including anharmonic effects (in a perturbative manner).[30] The resulting four contributions are distinguished by the superscript (n) for n-body effects and the index HZPE or AHZPE for the harmonic zero-point energy contributions and anharmonic corrections. We further improve the two-body harmonic ZPE contributions by including phonon-dispersion (PD) effects beyond the Einstein approximation for that term, named $E_{HZPE-PD}^{(2)}(V)$ [Eq. (3)].

$$E_{coh}^{dyn}(V) \cong E_{HZPE-E}^{(2)}(V) + E_{HZPE-E}^{(3)}(V) + E_{AHZPE}^{(2)}(V) + E_{AHZPE}^{(3)} + E_{HZPE-PD}^{(2)}(V) \tag{3}$$

Details of the calculation of the individual static and dynamic contributions can be found in the section *Computational Details*.

The results of our solid-state calculations for the fcc and hcp crystal structures are listed in Table 1 starting with the static two-body contributions $E^{(2)}$. Successively adding the additional terms of Equations (2) and (3) increases the accuracy of our results more and more. The table contains the fcc and hcp results for the lattice constant a, the corresponding volume V, the cohesive energy E_{coh}, and the bulk modulus B on the right and left, respectively. The last column lists the energetic difference between the two lattices. The lower part of the table shows the total results when the PS two-body potential or the Az potential is used instead of the JHBV potential, density-functional results, and experimental data.

The final lattice constant, cohesive energy, and bulk modulus are in excellent agreement with the experimental values with an unprecedented accuracy (deviation to the experimental value is at most $|\Delta E_{coh}| = 5$ J mol^{-1} and within the experimental error, $|\Delta a| = 0.003$ Å, $|\Delta B| = 2$ kbar, see discussion below). Note, to achieve such high accuracy, the four-body term is required despite its small size. In contrast to a previous study ($E^{(4)} = +65.4$ J mol^{-1} by Rościszewski et al.[13] as compared to our more accurate value of -7.7 J mol^{-1}) we now get the order of magnitude of this

Table 1: Static n-body energy $E^{(n)}(V)$ and zero-point vibrational energy $E_{ZPE}^{(n)}(V)$ contributions to the equilibrium lattice constant a (in Å), molar volume V (in cm^3 mol^{-1}), the cohesive energy E_{coh} (in J mol^{-1}), and bulk modulus B (in kbar) for fcc and hcp polymorphs are shown. The contributions of Equations (2) and (3) are successively added showing the convergence to the final results. The last column shows the difference in cohesive energies $\Delta E_{coh}^{fcc/hcp}$ between the fcc and hcp phase. The lower part of the table contains results obtained using the PS potential[33] and the Az potential[37] instead of the JHBV[32] potential as the underlying two-body potential, along with density functional results and experimental data.

Term	fcc				hcp				$\Delta E_{coh}^{fcc/hcp}$
	a	V	E_{coh}	B	a	V	E_{coh}	B	
$E^{(2)}$	5.2129	21.3266	−9200.16	37.322	3.6860	21.3259	−9201.37	37.328	1.21
$+E_{2C}^{(2)}$	5.2128	21.3259	−9201.42	37.328	3.6860	21.3252	−9202.63	37.333	1.21
$+E^{(3)}$	5.2571	21.8740	−8515.77	33.319	3.7173	21.8729	−8516.89	33.323	1.11
$+E^{(4)}$	5.2564	21.8648	−8523.43	33.353	3.7168	21.8641	−8524.15	33.355	0.72
$+E_{HZPE-E}^{(2)}$	5.3195	22.6619	−7710.52	27.939	3.7614	22.6613	−7711.19	27.942	0.67
$+E_{HZPE-PD}^{(2)}$	5.3163	22.6218	−7737.99	28.188	3.7599	22.6344	−7728.99	28.113	−9.00
$+E_{AHZPE}^{(2)}$	5.3156	22.6121	−7722.07	28.334	3.7594	22.6251	−7713.34	28.266	−8.73
$+E_{HZPE<M->E}^{(3)}$	5.3147	22.6006	−7717.22	28.372	3.7588	22.6137	−7708.43	28.302	−8.79
$+E_{AHZPE}^{(3)}$	5.3147	22.6013	−7717.47	28.361	3.7588	22.6146	−7708.66	28.155	−8.81
E_{coh}^{PS} [a]	5.3156	22.6123	−7705.88	28.224	3.7594	22.6247	−7696.84	28.183	−9.05
E_{coh}^{Az} [b]	5.3077	22.5116	−7709.02	28.107	3.7538	22.5242	−7699.81	28.090	−9.20
PBE[c]	5.7765	29.0185	−4044.9	12.05	4.0904	29.1439	−4021.6	12.02	−23.3
PBE-D2[c]	5.3212	22.6846	−11040.8	36.10	3.7632	22.6934	−11012.4	35.12	−28.4
PBE-D3[c]	5.4889	24.8969	−10418.2	24.90	3.8815	24.9019	−10378.3	24.45	−39.9
Expt.	5.3118[d]	22.564[d]	−7722(11)[e]	26.4[f]	3.7609[d]	22.652[d]			
Expt.	5.3002(1)[g]	22.416(1)[g]	−7724[h]	23.8(1.7)[i]					

[a] Taking the two-body terms for the PS potential instead (Ref. [33]). [b] Taking the two-body terms for the Az-potential instead but without the $E_{2C}^{(2)}$ term (Ref. [37]). [c] PBE results are without ZPE corrections. [d] X-ray diffraction data (Barrett and Meyer, Ref. [15]). [e] Thermodynamic data (Schwalbe et al., Ref. [39]). [f] Neutron scattering data (Batchelder et al., Ref. [40]). [g] X-ray diffraction data (Peterson et al., Ref. [38]). [h] Thermodynamic data (Pollack, Ref. [41]). [i] Neutron scattering data (Dorner et al., Ref. [42]).

term correct including the sign (which is negative in accordance with the Drude model that predicts an alternating series of n-body contributions in the long range). Further, to reach J mol^{-1} accuracy for the cohesive energy not only the two-body vibrational ZPE correction is important, but also anharmonicity effects and the corresponding three-body terms are required.

The accuracy of the individual n-body terms needs to be analyzed in more detail. Using a Lennard-Jones potential one can estimate the impact of the error in the two-body potential to the cohesive energy due to basis set incompleteness and limitations in the electron correlation procedure,[30] that is, $\Delta_{err}E_{coh} = 8.6093\,\Delta_{err}D_e$. A difference of 1.497 J mol^{-1} in the dissociation energy D_e between the JHBV and PS two-body potentials amounts to a difference of 12.9 J mol^{-1} in the cohesive energy in good agreement with our 11.6 J mol^{-1} value (see Table 1). However, the JHBV potential has a slightly larger dissociation energy, is closer to the empirical Az potential and perhaps therefore more accurate. Spin-orbit coupling is neglected in the two-body potential of Jäger et al.,[32] but is included in our calculations. These effects are of the order of 1 J mol^{-1} for the solid state and are therefore small, consistent with the remarks by Patkowski and Szalewicz.[33] The five-body term will be repulsive around the equilibrium geometry, and the two- to four-body contributions can be expected to be smaller than 1 J mol^{-1}. We therefore conclude that our accuracy in the cohesive energy is at least 10 J mol^{-1} (or better) and thus within the experimental error.

Concerning the structure, applying atmospheric pressure (101.325 kPa) lowers the lattice constant by only 4.5×10^{-5} Å and can therefore be neglected. Strictly, the two bond distances, theoretically and experimentally derived, cannot be directly compared, and in the limit of exact calculations differences can still be on the order of 10^{-3} Å.[43] Nevertheless, concerning the rather "large" discrepancy between the two available experimental values we suggest that new X-ray data is required. An accurate value for the equilibrium distance of the argon dimer from vibrational–rotational data would also be advantageous. The bulk modulus is difficult to measure and the deviation to our calculated value at 0 K may well be due to experimental errors.

Finally, we investigate the stability of the hcp vs. the fcc phase. It is well known that a simple Lennard-Jones potential stabilizes the hcp over the fcc phase.[44] Table 1 shows that this is also the case for the two-body potential used here, albeit by a very small amount of 1.2 J mol^{-1}. Adding three- and four-body contributions and even ZPE corrections within the Einstein approximation does not change this situation significantly. Only the coupling of the vibrational modes in the solid, that is, the phonon dispersion finally brings the fcc phase significantly below the hcp phase in energy. This results in a preference of the fcc over the hcp phase by only 8.8 J mol^{-1}, which is obviously large enough to stabilize the fcc phase, in contrast to Ostwald's step rule. In fact, if we take the two-body contribution only and add phonon dispersion, the fcc phase is stabilized by 12.1 J mol^{-1} compared to the hcp structure. Moreover, at finite temperatures the fcc phase has higher entropy than the hcp phase.[45]

The density functionals used in this study (see Table 1) cannot reproduce the difference correctly (nor will other common functionals do so, in our opinion) even when dispersion corrections are included, which needs to be investigated further. Of course, the rare-gas solids are really special cases ideally suited for the quantum chemical many-body treatment used in this work.

We finally mention that the metastable hcp phase has been observed for freshly frozen argon by Barrett and Meyer.[15,16] They report an ideal $c/a \approx 6.142_9/3.760_9 \approx \sqrt{8/3}$ ratio for the lattice constants, and their lattice constant a is in excellent agreement with our value of $a = 3.7588$ Å.

To conclude, we produced $J\,mol^{-1}$ accuracy for the cohesive energy of argon and correctly predicted the energy separation between the fcc and hcp phase. We have thus come a long way since the very first ab initio treatment of crystalline systems by Löwdin.[46,47] Our next challenge will be to apply this many-body treatment to the heavier rare gases as well as to molecular crystals at finite temperatures and pressures. Work in this direction is underway.

Computational Details

For all solid-state calculations we used our program SAMBA.[30] The many-body expansion of the static part of the total cohesive energy $E_{coh}^{stat}(V)$ per atom (utilizing translational symmetry) at a certain volume V is defined as,[30,48]

$$E_{coh}^{stat}(V) = \sum_{k=2}^{n} E^{(k)}(V) \cong \frac{1}{2}\sum_{i=1}^{N_2} \Delta E^{(2)}(R_{0i}) + \frac{1}{3}\sum_{i=1}^{N_3}\sum_{j>i}^{N_3}(R_{0i}, R_{0j}, R_{ij})$$
$$+ \frac{1}{4}\sum_{i=1}^{N_4}\sum_{j>i}^{N_4}\sum_{k>j>i}^{N_4} \Delta E^{(4)}(R_{0i}, R_{0j}, R_{0k}, R_{ij}, R_{ik}, R_{jk}) + \ldots \quad (4)$$

Note that the expression on the right-hand side is already an approximation to the cohesive energy because we restrict the sums to a finite number of atoms, N_2, N_3, and N_4, that are included in the evaluations of two-, three-, and four-body terms, respectively. We can further truncate the above expression if the convergence is fast with increasing order n. The expansion becomes exact for n and $N_i \to \infty$.[19] $\Delta E^{(k)}$ stands for the k-body energy contribution to the total energy coming from the k-body fragments with internuclear distances R_{ij} between the atoms i and j for a certain lattice volume V. The (arbitrarily chosen) central atom is denoted by the index 0. For the two-body potential we used the analytical pair potential of Jäger et al. (JHBV) which contains electron correlation up to CCSDT(Q) level of theory and scalar relativistic effects (for details see Ref. [32,49]). Spin-orbit contributions were taken from X2C/CCSD(T) calculations[50] and fitted to the following analytical form (derived from the London dispersion formula) [Eq. (5)]

$$\Delta E_{SO}^{(2)}(R_{ij}) = -C_{SO}R_{ij}^{-6} \quad (5)$$

with $C_{SO} = 3.81 \times 10^{-3}$ a.u. and R_{ij} being the internuclear distance of the dimer with atoms i, j. For the three-body potential we took the potential of Cencek et al. evaluated at the CCSDT(Q) level of theory including scalar relativistic

effects.[34] For neon it was shown that already the classical triple-dipole (Axilrod-Teller) term is a good approximation in the long range. Hence we chose the four-body contribution derived from the classical Drude model[35,36,51,52] as the fourth-order dipole–dipole term ($\Delta E^{(4)} \cong \Delta E_{DD}^{(4)}$) for the four-body fragment containing atoms i, j, k, and l [Eq. (6)]

$$\Delta E_{DD}^{(4)}(ijkl) = \omega[f(ijkl) + f(ijlk) + f(ikjl)] \quad (6)$$

with

$$f(ijkl) = (R_{ij}R_{jk}R_{kl}R_{il})^{-3}[(\vec{u}_{ij} \cdot \vec{u}_{jk})^2 + (\vec{u}_{ij} \cdot \vec{u}_{kl})^2 + (\vec{u}_{ij} \cdot \vec{u}_{li})^2$$
$$+ (\vec{u}_{jk} \cdot \vec{u}_{kl})^2 + (\vec{u}_{jk} \cdot \vec{u}_{li})^2 + (\vec{u}_{kl} \cdot \vec{u}_{li})^2$$
$$- 3(\vec{u}_{ij} \cdot \vec{u}_{jk})(\vec{u}_{ij} \cdot \vec{u}_{kl})(\vec{u}_{kl} \cdot \vec{u}_{ij}) - 3(\vec{u}_{ij} \cdot \vec{u}_{jk})(\vec{u}_{jk} \cdot \vec{u}_{li})(\vec{u}_{li} \cdot \vec{u}_{ij})$$
$$- 3(\vec{u}_{ij} \cdot \vec{u}_{kl})(\vec{u}_{kl} \cdot \vec{u}_{li})(\vec{u}_{li} \cdot \vec{u}_{ij}) - 3(\vec{u}_{jk} \cdot \vec{u}_{kl})(\vec{u}_{kl} \cdot \vec{u}_{li})(\vec{u}_{li} \cdot \vec{u}_{jk})$$
$$+ 9(\vec{u}_{ij} \cdot \vec{u}_{jk})(\vec{u}_{jk} \cdot \vec{u}_{kl})(\vec{u}_{kl} \cdot \vec{u}_{li})(\vec{u}_{li} \cdot \vec{u}_{ij}) - 1] \quad (7)$$

where $\vec{u}_{ij}$ is the unit vector in direction from atom i to atom j. The prefactor ω was chosen according to Johnsson and Spurling (corrected for a missing factor of 8),[51] that is, $\omega = -(45/32)ca^4$ with a scaling factor[53] $c = 0.6963$ and the dipole polarizability $\alpha = 11.07$ a.u. taken from experimental measurements.[54,55] The Drude long-range behavior of the four-body potential was verified through scalar relativistic CCSD(T) calculations[56] using Dunning's correlation consistent augmented triple-zeta basis set[57] adjusted for Douglas-Kroll calculations[58] including counter-poise corrections[59] for the basis set superposition error. A full active orbital space was taken in the all-electron correlation treatment. Note that convergence of the coupled cluster energy to $< 10^{-9}$ a.u. was required to obtain stable results in the bonding region for the four-body potential.

In order to get the static part of the cohesive energy from Equation (4) with the desired accuracy, we sum over $N_2 \sim 700\,000$ atoms in the two-body part, $N_3 \sim 67\,500$ atoms in the three-body part and $N_4 \sim 7500$ atoms in the four-body part. As the computation of the n-body terms becomes computationally very demanding with increasing order n, that is $\sim O(N^{n-1})$, we had to decrease the numbers of atoms included with increasing n. However, we checked that each term is converged within a range of less than 0.01 $J\,mol^{-1}$.

The harmonic zero-point vibrational crystal energy (ZPE) contribution was evaluated for the two-body potential[60] [Eq. (8)].

$$E_{HZPE-E}^{(2)} + E_{HZPE-PD}^{(2)} = \frac{1}{2N}\sum_{\vec{k},i} \hbar\,\omega_i(\vec{k}) \quad (9)$$

The dynamic matrices for the fcc and hcp structures were constructed and diagonalized in reciprocal space to obtain the frequencies $\omega_i(\vec{k})$, using a grid of k points homogeneously distributed in the Brillouin zone, and large enough to converge the zero-point energy to less than 1 $J\,mol^{-1}$. The three-body ZPE contribution was evaluated within the Einstein approximation moving the central atom in the two- and three-body field of all other atoms (see the discussion in Ref. [22]). Finally the anharmonic corrections were obtained

from perturbation theory of the internal force field up to fourth order within the Einstein approximation.[30]

The bulk modulus B was obtained from the volume-dependent increments in Equation (2) using $B = V^{-1}d^2E/dV^2$. The numerical stability of our procedure has been tested and is < 0.0001 Å for the lattice constant, < 0.1 J mol^{-1} for the cohesive energy, and < 0.1 kbar for the bulk modules (note the values given are shown with more significant figures to highlight the differences in the fcc and hcp structures). The recommended mass of 39.948 amu for argon was chosen (the difference in the ZPEs by taking the 40-Ar mass instead can be neglected). We also performed density functional calculations as implemented in the VASP package, using a plane-wave basis set (cut-off energy $E_c = 800$ eV) and the standard projector-augmented wave (PAW) datasets for argon with a k-space sampling of $(7 \times 7 \times 7)$ using the Monkhorst-Pack scheme.[61] The electron–electron interaction was modeled within the generalized gradient approximation to the exchange-correlation energy functional[62] including Grimme's dispersion corrections (PBE-D2[63] and PBE-D3).[64–66] Very tight convergence criteria for SCF convergence (10^{-10} eV) and structure optimization (5×10^{-3} eV Å^{-1}) were chosen.

Acknowledgements

[1] R. J. Bartlett, *J. Phys. Chem.* **1989**, *93*, 1697.
[2] K. L. Bak, P. Jørgensen, J. Olsen, T. Helgaker, W. Klopper, *J. Chem. Phys.* **2000**, *112*, 9229–9242.
[3] A. D. Boese, M. Oren, O. Atasoylu, J. M. L. Martin, M. Kállay, J. Gauss, *J. Chem. Phys.* **2004**, *120*, 4129–4141.
[4] A. Tajti, P. G. Szalay, A. G. Császár, M. Kállay, J. Gauss, E. F. Valeev, B. A. Flowers, J. Vázquez, J. F. Stanton, *J. Chem. Phys.* **2004**, *121*, 11599–11613.
[5] M. E. Harding, J. Vázquez, J. Gauss, J. F. Stanton, M. Kállay, *J. Chem. Phys.* **2011**, *135*, 044513.
[6] P. Fulde, *Electron Correlations in Molecules and Solids*, Springer, Heidelberg, **1995**.
[7] T. Bučko, J. Hafner, S. Lebègue, J. G. Ángyán, *J. Phys. Chem. A* **2010**, *114*, 11814–11824.
[8] G. H. Booth, A. Grüneis, G. Kresse, A. Alavi, *Nature* **2013**, *493*, 365–370.
[9] J. Yang, W. Hu, D. Usvyat, D. Matthews, M. Schütz, G. K.-L. Chan, *Science* **2014**, *345*, 640–643.
[10] X. Liu, P. Müller, P. Kroll, R. Dronskowski, W. Wilsmann, R. Conradt, *ChemPhysChem* **2003**, *4*, 725–731.
[11] J. Maddox, *Nature* **1988**, *335*, 201.
[12] It is not possible to predict crystal structures purely from chemical intuition except for the simplest and most obvious cases.
[13] K. Rościszewski, B. Paulus, P. Fulde, H. Stoll, *Phys. Rev. B* **2000**, *62*, 5482–5488.
[14] S. Y. Willow, M. A. Salim, K. S. Kim, S. Hirata, *Sci. Rep.* **2015**, *5*, 14358.
[15] C. S. Barrett, L. Meyer, *J. Chem. Phys.* **1964**, *41*, 1078–1081.
[16] L. Meyer, C. S. Barrett, P. Haasen, *J. Chem. Phys.* **1964**, *40*, 2744–2745.
[17] H. Stoll, *Phys. Rev. B* **1992**, *46*, 6700–6704.
[18] B. Paulus, *Phys. Rep.* **2006**, *428*, 1.
[19] A. Hermann, R. P. Krawczyk, M. Lein, P. Schwerdtfeger, I. P. Hamilton, J. J. P. Stewart, *Phys. Rev. A* **2007**, *76*, 013202.
[20] N. Gaston, B. Paulus, K. Rościszewski, P. Schwerdtfeger, H. Stoll, *Phys. Rev. B* **2006**, *74*, 094102.
[21] H. Stoll, K. Doll, *Chem. Phys. Lett.* **2011**, *501*, 283–286.
[22] K. Rościszewski, B. Paulus, *Phys. Rev. B* **2002**, *66*, 092102.
[23] E. Pahl, F. Calvo, L. Koči, P. Schwerdtfeger, *Angew. Chem. Int. Ed.* **2008**, *47*, 8207–8210; *Angew. Chem.* **2008**, *120*, 8329–8333.
[24] P. Schwerdtfeger, A. Hermann, *Phys. Rev. B* **2009**, *80*, 064106.
[25] J. Wiebke, E. Pahl, P. Schwerdtfeger, *Angew. Chem. Int. Ed.* **2013**, *52*, 13202–13205; *Angew. Chem.* **2013**, *125*, 13442–13446.
[26] B. Jäger, R. Hellmann, E. Bich, E. Vogel, *J. Chem. Phys.* **2011**, *135*, 084308.
[27] J. Wiebke, P. Schwerdtfeger, G. E. Moyano, E. Pahl, *Chem. Phys. Lett.* **2011**, *514*, 164–167.
[28] J. Wiebke, P. Schwerdtfeger, E. Pahl, *J. Chem. Phys.* **2012**, *137*, 064702.
[29] B. Jäger, *Z. Phys. Chem.* **2013**, *227*, 303–314.
[30] P. Schwerdtfeger, N. Gaston, R. P. Krawczyk, R. Tonner, G. E. Moyano, *Phys. Rev. B* **2006**, *73*, 064112.
[31] J. Moellmann, S. Grimme, *J. Phys. Chem. C* **2014**, *118*, 7615–7621.
[32] B. Jäger, R. Hellmann, E. Bich, E. Vogel, *Mol. Phys.* **2009**, *107*, 2181–2188.
[33] K. Patkowski, K. Szalewicz, *J. Chem. Phys.* **2010**, *133*, 094304.
[34] W. Cencek, G. Garberoglio, A. H. Harvey, M. O. McLinden, K. Szalewicz, *J. Phys. Chem. A* **2013**, *117*, 7542–7552.
[35] W. L. Bade, *J. Chem. Phys.* **1957**, *27*, 1280–1284.
[36] W. L. Bade, *J. Chem. Phys.* **1958**, *28*, 282–284.
[37] R. A. Aziz, *J. Chem. Phys.* **1993**, *99*, 4518–4525.
[38] O. G. Peterson, D. N. Batchelder, R. O. Simmons, *Phys. Rev.* **1966**, *150*, 703–711.
[39] L. A. Schwalbe, R. K. Crawford, H. H. Chen, R. A. Aziz, *J. Chem. Phys.* **1977**, *66*, 4493–4502.
[40] D. N. Batchelder, M. F. Collins, B. C. G. Haywood, G. R. Sidey, *J. Phys. C* **1970**, *3*, 249–255.
[41] G. L. Pollack, *Rev. Mod. Phys.* **1964**, *36*, 748–791.
[42] B. Dorner, H. Egger, *Phys. Status Solidi B* **1971**, *43*, 611–617.
[43] M. Hargittai, I. Hargittai, *Int. J. Quantum Chem.* **1992**, *44*, 1057–1067.
[44] B. W. van de Waal, *Phys. Rev. Lett.* **1991**, *67*, 3263–3266.
[45] A. Travesset, *J. Chem. Phys.* **2014**, *141*, 164501.
[46] P. Löwdin, *J. Chem. Phys.* **1951**, *19*, 1570–1578.
[47] P. Löwdin, *J. Chem. Phys.* **1951**, *19*, 1579–1591.
[48] I. G. Kaplan, R. Santamaria, O. Novaro, *Mol. Phys.* **1995**, *84*, 105–114.
[49] B. Jäger, R. Hellmann, E. Bich, E. Vogel, *Mol. Phys.* **2010**, *108*, 105.
[50] DIRAC, a relativistic ab initio electronic structure program, Release DIRAC14 (**2014**), written by T. Saue, L. Visscher, H. J. Aa. Jensen, and R. Bast with contributions from V. Bakken, K. G. Dyall, S. Dubillard, U. Ekström, E. Eliav, T. Enevoldsen, E. Faßhauer, T. Fleig, O. Fossgaard, A. S. P. Gomes, T. Helgaker, J. K. Lærdahl, Y. S. Lee, J. Henriksson, M. Ilias, Ch. R. Jacob, S. Knecht, S. Komorovsky, O. Kullie, C. V. Larsen, H. S. Nataraj, P.

12204 www.angewandte.org

© 2016 Wiley-VCH Verlag GmbH & Co. KGaA, Weinheim

Angew. Chem. Int. Ed. **2016**, *55*, 12200–12205

Norman, G. Olejniczak, J. Olsen, Y. C. Park, J. K. Pedersen, M. Pernpointner, R. di Remigio, K. Ruud, P. Sałek, B. Schimmelp-fennig, J. Sikkema, A. J. Thorvaldsen, J. Thyssen, J. van Stralen, S. Villaume, O. Visser, T. Winther, S. Yamamoto (see http://www.diracprogram.org).

[51] C. H. J. Johnson, T. H. Spurling, *Aust. J. Chem.* **1974**, *27*, 241 – 247.

[52] M. Rigby, E. Smith, W. Wakeham, G. Maitland, *The Forces Between Molecules*, Oxford Science, New York, **1986**.

[53] M. A. V. der Hoef, P. A. Madden, *Mol. Phys.* **1998**, *94*, 417 – 433.

[54] U. Hohm, K. Kerl, *Mol. Phys.* **1990**, *69*, 803 – 817.

[55] U. Hohm, K. Kerl, *Mol. Phys.* **1990**, *69*, 819 – 831.

[56] Gaussian09 (Revision D.01), M. J. Frisch, G. W. Trucks, H. B. Schlegel, G. E. Scuseria, M. A. Robb, J. R. Cheeseman, G. Scalmani, V. Barone, B. Mennucci, G. A. Petersson, H. Nakat-suji, M. Caricato, X. Li, H. P. Hratchian, A. F. Izmaylov, J. Bloino, G. Zheng, J. L. Sonnenberg, M. Hada, M. Ehara, K. Toyota, R. Fukuda, J. Hasegawa, M. Ishida, T. Nakajima, Y. Honda, O. Kitao, H. Nakai, T. Vreven, J. A. Montgomery, Jr., J. E. Peralta, F. Ogliaro, M. Bearpark, J. J. Heyd, E. Broth- ers, K. N. Kudin, V. N. Staroverov, R. Kobayashi, J. Normand, K. Raghavachari, A. Rendell, J. C. Burant, S. S. Iyengar, J. Tomasi, M. Cossi, N. Rega, J. M. Millam, M. Klene, J. E. Knox, J. B. Cross, V. Bakken, C. Adamo, J. Jaramillo, R. Gomperts, R. E. Stratmann, O. Yazyev, A. J. Austin, R. Cammi, C. Pomelli, J. W. Ochterski, R. L. Martin, K. Morokuma, V. G. Za- krzewski, G. A. Voth, P. Salvador, J. J. Dannenberg, S. Dapprich, A. D. Daniels,. Farkas, J. B. Foresman, J. V. Ortiz, J. Cioslowski, D. J. Fox, Gaussian Inc. Wallingford CT **2009**.

[57] D. E. Woon, T. H. Dunning, *J. Chem. Phys.* **1993**, *98*, 1358 – 1371.

[58] T. Nakajima, K. Hirao, *Chem. Rev.* **2012**, *112*, 385 – 402.

[59] S. F. Boys, F. Bernardi, *Mol. Phys.* **1970**, *19*, 553.

[60] G. E. Moyano, P. Schwerdtfeger, K. Rościszewski, *Phys. Rev. B* **2007**, *75*, 024101.

[61] P. E. Blöchl, *Phys. Rev. B* **1994**, *50*, 17953.

[62] J. P. Perdew, K. Burke, M. Ernzerhof, *Phys. Rev. Lett.* **1996**, *77*, 3865.

[63] S. Grimme, *J. Comput. Chem.* **2006**, *27*, 1787 – 1799.

[64] S. Grimme, J. Antony, S. Ehrlich, H. Krieg, *J. Chem. Phys.* **2010**, *132*, 154104.

[65] S. Grimme, *WIRE: Comput. Mol. Sci.* **2011**, *1*, 211 – 228.

[66] G. Sun, J. Krti, P. Rajczy, M. Kertesz, J. Hafner, G. Kresse, *J. Mol. Struct. THEOCHEM* **2003**, *624*, 37 – 45.